AIAA JOURNAL
Vol. 32, No. 3, March 1994

Flowfield Measurements in Supersonic Film Cooling Including the Effect of Shock-Wave Interaction

K. A. Juhany* and M. L. Hunt†
California Institute of Technology, Pasadena, California 91125

A study has been made to investigate the flowfield of supersonic slot injection and its interaction with a two-dimensional shock wave. Air and helium were injected at Mach numbers of approximately 1.3 and 2.2 into an airstream of Mach 2.4. Measurements of the total pressure profiles perpendicular to the wall were made at several axial locations, the farthest being at 90 slot heights. The profiles provided details of the structure of the flow for the different injection conditions. With heated gas injection, experiments were conducted to determine the adiabatic wall temperatures and the wall static pressures. These measurements were then repeated with the impingement of two-dimensional shock waves at 60 slot heights downstream of the slot. The shock strengths were chosen to illustrate the differences between separated and attached flows. The shock strength that produced incipient separation was found to be smaller when helium was injected than when no film coolant was present. Conversely, the shock strength that produced incipient separation with air injection was slightly larger than that obtained without film cooling.

Introduction

SUPERSONIC and hypersonic vehicles are subjected to severe aerodynamic heating. Aerodynamic heating is particularly serious in the interior of a vehicle's engine where a combination of viscous dissipation, shock-wave interactions, and combustion-induced heating are present.[1] In a scramjet engine, the hydrogen fuel will also serve as a coolant[2] using a combination of film cooling and internal convective cooling. In the film-cooling scheme, cold hydrogen would flow through channels in the engine's structure and then would be injected through a slot parallel to the main stream.[3] The cold injected hydrogen serves as a thermal buffer between the main stream environment and the wall. Film cooling represents an attractive scheme for active cooling since it is simple to construct, adds thrust to the engine, energizes the boundary layer to prevent separation, and reduces heating.

To apply such a method to a scramjet engine, one needs appropriate correlations that include the effect of shock-wave impingement to calculate the required film coolant design parameters. To improve film-cooling predictions, more experiments are required to better understand the physical nature of film-cooling flows in high-speed environments. Few studies have examined supersonic film cooling,[4] especially with shock-wave interaction. Results of previous studies provide limited and contradicting information, so that concrete conclusions are difficult to obtain.

Background

Film cooling in low-speed flows has been thoroughly investigated as reviewed by Goldstein.[5] The aim of these investigations is to develop a correlation for effectiveness, which in a low-speed flow is defined as

$$\eta = \frac{T_w(x) - T_\infty}{T_i - T_\infty} \tag{1}$$

where T_w, T_∞, and T_i are the temperature of the wall for adiabatic conditions, the freestream temperature, and the injectant temperature, respectively. Experimental measurements have been used to develop relations for effectiveness as a function of downstream position divided by slot height x/s and the ratio of mass flux for the injected flow to that in the freestream, $\lambda = (\rho u)_i/(\rho u)_\infty$. The physical basis for these relations has also been motivated from simple integral analysis of the flowfield.[5]

The variation in the effectiveness with downstream position is accompanied by changes in flowfield structure. Some subsonic film-cooling experiments[6] and other subsonic experiments involving wall jets with moving freestream[7] have shown that the flowfield can be divided into three regions: a potential core region, a wall-jet region, and a boundary-layer region. The potential core region, like a freejet, contains a viscous layer that emanates from the lip and ends when it meets the slot-flow boundary layer. In this region the wall temperature remains at a constant value equal to that of the injected fluid (in the case of subsonic injection) or equal to the recovery value (in the case of supersonic injection). Thus, the effectiveness in the potential core region is unity. The wall-jet region starts when the viscous layer emanating from the lip merges with the injectant boundary layer. In this region intense mixing takes place, and the wall temperature increases toward the freestream value. In the boundary-layer region, the flow then relaxes to that of a boundary layer. Consequently, the effectiveness decreases from unity near the injector and approaches zero far downstream. Thus, film-cooling flows combine different types of familiar flows: a freejet flow, a wake, a shear layer, and a boundary layer.

The different hydrodynamic features of the flow in each region suggest using different scaling laws to predict effectiveness. This approach was attempted with some success in low-speed flow,[8] where empirical data from jet flows and boundary-layer flows were applied for near and far regions, respectively. These approximate flowfields were used in the energy equation to solve for the distribution in wall temperature and the film-cooling effectiveness. In these incompressible analyses, the thermodynamic properties were considered invariant within the flowfield.[5]

The film-cooling effectiveness in high-speed flow is often defined as

$$\eta = \frac{T_{rw}(x) - T_{r\infty}}{T_{ri} - T_{r\infty}} \tag{2}$$

where the subscript r indicates the recovery temperatures measured for adiabatic conditions. To correlate the data in high-speed flow, previous studies attempted to use modified incompressible flow correlations.[5] However, these correlations were not successful in predicting experimental measurements.

Presented as Paper 92-2950 at the AIAA 27th Thermophysics Conference, Nashville, TN, July 6–8, 1992; received Feb. 2, 1993; revision received Aug. 13, 1993; accepted for publication Aug. 13, 1993.

*Research Assistant, Aeronautics Department. Student Member AIAA.
†Assistant Professor, Mechanical Engineering Department. Member AIAA.

The extension of the incompressible results to supersonic flow is complicated by two issues that are characteristic of high-speed flows: the strong coupling between the momentum and energy equation and the appearance of shock waves. As a consequence of the strong coupling between the momentum and energy equations, the thermal features of the flow are strongly influenced by the hydrodynamic aspects. In addition, the presence of shock waves in supersonic film-cooling applications may enhance mixing between the freestream and the film coolant, and if the shock waves are of sufficient strength, the flow may separate. Most high-speed film-cooling correlations, however, have evolved from those for incompressible flows and little work has focused on improving the correlations by determining the flow structure. Some information on the film-cooling flowfield and the effects of shock-wave interaction can be gleaned from related studies on tangential slot injection for boundary-layer control and for fuel mixing.

In the area of boundary-layer control, tangential slot injection has been employed as a mechanism to prevent shock-induced separation.[9] The addition of momentum from the slot flow enables the boundary layer to withstand the adverse pressure gradient caused by the shock waves. In some of the early work by Peak,[10] an air-air experiment was used with a freestream Mach number of 1.8, an isoenergetic injection of Mach number 2.37, and a mass flux ratio of $\lambda = 0.6-1.5$ to investigate the effect of injection to prevent shock-wave/turbulent-boundary-layer-induced separation. By varying the shock strength and the distance from the slot to the location of the shock-wave impingement, Peak concluded that the optimum position of the injectant was a distance of about six times the thickness of the freestream boundary layer upstream of the shock-impingement location,[10] which corresponds to 16 slot heights. By probing the flowfield, Peak arrived at two criteria for boundary-layer control. The first is that the minimum total pressure in the wake of the slot lip must be greater than the local static pressure to prevent flow reversal; the second is that the decrease in the peak total pressure of the jet must be gradual so that the new wall boundary layer is not separated. Peak's profiles were obtained in the potential core region of the flowfield ($x/s \leq 33$).

The effect of molecular weight of the injectant on shock-wave/boundary-layer control was investigated by Grin and Zakharov.[11] Helium and air were injected at sonic velocities into an airstream at Mach 6. The injection was situated near or within the separation zone. Their work indicated that when helium was injected at the same momentum flux as air, helium was inferior to air in preventing separation. However, when helium was injected at the same mass-flux ratio as air, the helium and air were equally effective. Grin and Zakharov attribute the inferiority of helium at matched momentum flux to the associated increase in the pressure mismatch between the injectant and the freestream in the case of helium injection.[11]

In the area of fuel injection, one possible method of injection into supersonic flow is injection parallel to the wall. The advantage of using parallel injection, as opposed to the more mixing-efficient angled injection, is to avoid large momentum losses associated with angled injection.Yates provides detailed flowfield information on supersonic hydrogen slot injection of Mach 1.2 flow in an airstream of Mach 2.1 ($\lambda = 0.088$ and 0.120). The probing was limited to three locations, the farthest being at 30 slot heights downstream of the injection slot.[12] Other work by Walker et al.[13] and Hyde et al.[14] used the same wind-tunnel model with freestream Mach number of 2.9 and an injectant Mach number of 1.7. Walker et al.[13] studied an isoenergetic injection, whereas Hyde et al.[14] also used heated injection. Both mean and turbulent profiles were measured at four locations, the farthest being 20 slot heights downstream. A shock wave of pressure ratio 1.8 was generated in the flow to investigate the interaction with the slot flow at about 15 slot heights downstream. The interaction between the shock wave and the injectant produced an increase in the viscous-layer thickness and the turbulence intensity. Kwok et al.[15] tested helium injection in the same wind tunnel and compared the results with those for air injection. These results show that helium mixed more efficiently than air when injected at the same Mach number. In these studies the major concern was to examine the mixing between the slot flow and freestream, and hence the measurements dealt with the growth rate and the trajectory of the mixing layer. The experiments did not present measurements such as adiabatic wall temperature or wall heat flux that could be used to evaluate effectiveness. In addition, these studies have used large slot heights compared with the incoming boundary layer, which is not typical of the film-cooling application.

Fewer studies have examined shock-wave and film-coolant interactions to determine the effect on the film-cooling effectiveness. Some early work by Alzner and Zakkay[16,17] and Ledford and Stollery[18] has shown that the film coolant can reduce the heat transfer rise in the shock-wave interaction region. However, in an air-helium experiment, with a freestream Mach number of 6.4, injectant Mach number of 3.0, and a maximum mass-flux ratio of $\lambda = 0.25$, Holden et al.[19] and Olsen et al.[20] indicated that shock waves degrade film cooling to the point at which the coolant is not effective after the interaction. Furthermore, it was found that injection can induce separation. They compared their results with those of Alzner and Zakkay[16,17] ($Ma_\infty = 6.0$ and $Ma_j = 1.0$) and indicated a discrepancy between their results and those of Alzner and Zakkay.[17] However, the disparity results from the difference in slot location relative to the shock-wave impingement location. The results of Alzner and Zakkay,[17] used for comparison by Holden et al.,[19] involved a slot located within the separation bubble just upstream of the recompression point. This location is where the peak heating occurs for a shock-wave/boundary-layer interaction. The results of Holden et al.[19] were for a slot located at approximately 60 or 90 slot heights, depending on the slot height used. A comparison of the results of Holden et al.[19] and Alzner and Zakkay[16] at the location in which the injection occurred just upstream of the interaction indicates similar trends in both pressure and heat transfer.

The general conclusion obtained from previous shock-wave/slot-injectant interaction is that slot injection seems to prevent shock-wave-induced separation as long as the injection is at a sufficient blowing rate and is near the shock-wave impingement location. The conflict between previous studies seems to be in the area where the shock-wave impingement location is away from the slot, in the wall-jet region or the boundary-layer region. The knowledge of the type of the film-cooling flow would provide better understanding of the shock-injectant interaction process. However, most previous studies did not include flow profiles at the location of shock-wave impingement.

Juhany et al.[4] obtained effectiveness data for both helium and air injection for several injection Mach numbers between sonic conditions and Mach 2.2. The freestream and the injectant pressures were matched, and the freestream Mach number was 2.4. The instrumented wall was insulated to provide a controlled boundary condition. The results indicate, as in other studies, that the length over which high effectiveness is maintained increases with increasing mass-flux ratio and increases for gases with higher specific heat. Using the definition given by Eq. (2), the study also indicated that effectiveness of better than 80% was obtained for distances greater than or equal to 65 slot heights. Therefore, the effects of shock waves on the film cooling are also of interest in other locations besides those near the slot.

In this paper, the effect of shock-wave interaction with slot injection is investigated for a region of the flow in which the film-cooling effectiveness is close to unity. As in a previous film-cooling study,[4] the effects of the injectant Mach number and the specific heat of the injectant are explored. The strength of the shock that impinges on the flow is varied so that the wall temperatures and pressures can be determined for conditions with and without flow separation.

Experimental Facility

The experiments were conducted in the Graduate Aeronautical Laboratory, California Institute of Technology (GALCIT), continuous supersonic wind tunnel. Figure 1 shows a schematic of half-nozzle configuration used in the slot-injection experiments. Air enters the wind tunnel at ambient pressure and temperature. At the beginning of the test rhombus where the injectant slot is located, the

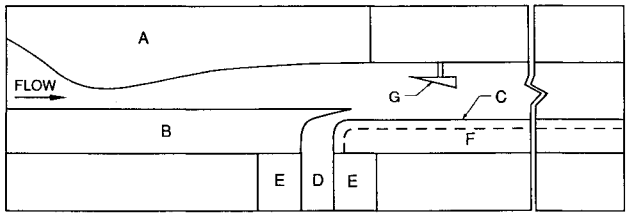

Fig. 1 Schematic of wind-tunnel test section (drawing not to scale).

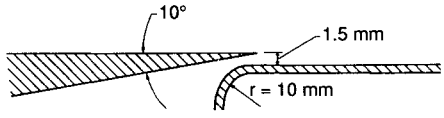

Fig. 2 Injection nozzle geometry (drawing not to scale).

boundary layer is turbulent with a thickness of 3.4 mm, a displacement thickness of 1.2 mm, a momentum thickness of 0.27 mm, and a Reynolds number/m of 9.0×10^6. The nominal freestream Mach number is 2.44 ± 0.02. The total test-section length, span, and height are 400, 65, and 26 mm, respectively.

The injected gas is supplied from compressed gas bottles that are connected to a manifold and a pressure regulator. The regulator is used to adjust the pressure of the injectant before it enters the turbine flow meter. Using the flow meter, the uncertainty in the mass flow measurements is approximately 5%, with the largest values occurring at the highest flow rates. The heating of the injectant is accomplished using electrical heating tapes wrapped around the copper pipes. After the heating of the flow, the flow is throttled and then enters the injection reservoir where the total temperature and total pressures are measured. Figure 2 shows the geometry of the injection nozzle; the slot height at the exit of the injection nozzle is 1.5 mm.

The 2-mm-thick instrumented plate is made from Hastelloy-X, a low thermal conductivity nickel-cobol alloy used to reduce conduction from the injection slot to the downstream section and from the plate sides. To minimize heat transfer from the instrumented plate to the exterior, the region behind the plate is open to the low-pressure downstream environment of the tunnel. Thermocouples are mounted on the back side of the plate into 1-mm holes drilled 0.3 mm below the surface. Most thermocouples are located close to the centerline of the plate; however, every fourth thermocouple is placed closer to the side walls to assess the heat loss. The temperature difference between that at the centerline and that at the side walls was at most 3°C; as a result, the temperatures were not corrected for losses to the environment, and all of the temperature measurements are included in the presented results. The plate also contains pressure taps that are connected to piezoelectric transducers. The pressure transducers have a range of 0–260 Pa and an accuracy of 1% of full scale. All thermocouples and pressure transducers are connected to a PC-based data acquisition system.

The pitot probe is a boundary-layer cobra-type probe, fabricated from 1.58-mm-o.d. 316 stainless steel tubing with the tip flattened and then filed to 0.20×2 mm and an opening of 0.1 mm. The pitot probe is pitched upwards at an angle of about 10 deg to the freestream direction, allowing the probe to approach the wall with minimum disturbance to the flow. The probe holder can be located at five fixed positions in the wind tunnel. The probe is traversed perpendicular to the wall by means of a high-precision microhead traversing mechanism located under the test section. A linear potentiometer is attached to the traversing mechanism, which in turn is connected to the data acquisition system to record the position of the probe.

On the wall opposite the instrumented plate is a movable wedge that is used to generate a two-dimensional oblique shock wave. The wedge angle may be continuously varied to the desired shock strength, and the location of the wedge can be placed in several axial positions. To insure a two-dimensional shock interaction, the span of the wedge is less than that of the wind tunnel by half a boundary-layer thickness on each side. In addition, the large ratio of test section span to height (2.5) lessens the influence of any entrained fluid (from the side wall boundary layer) on the instrumented section of the plate.

Before each wind-tunnel startup and shutoff, the wedge was positioned at zero angle of attack to prevent it from damage due to aerodynamic loading. The angle of the wedge was positioned while the wind tunnel was operating, but this angle of attack was not measured because of the limited accuracy of the measurement. Instead, it was decided that the strength of the shock be determined by the pressure jump observed on the wall. When shock interaction with injection was being investigated, the injectant was turned off and the wall pressure distribution was checked to determine the shock strength.

In the present experiments, the impact-probe profiles were measured for the isoenergetic injection of both helium and air (at a total temperature equal to that of the freestream, $T_{ti} = T_{t\infty} \approx 300$ K). The injection Mach numbers were $M_i = 1.3$ and 2.2 for helium and $M_i = 1.2$ and 2.2 for air. The static pressure in the injected flow matched that in the freestream. For the film-heating experiments, the injected gas was heated to temperatures ranging from $T_{ti} = 335$ to 425 K. Table 1 presents the range of injection parameters for the heated and unheated conditions. The table also includes the momentum flux ratio $(\rho u^2)_i/(\rho u^2)_\infty$ and the slot Reynolds number Re_s based on the injection Mach number, injection temperature, and slot height. All of the wall temperature measurements were obtained after the instrumented plate reached thermal equilibrium.

Air and Helium Injection Profiles

Preliminary runs were made to investigate the two dimensionality of the injectant flow. The pitot pressure profiles of the injectant obtained at three spanwise locations were identical. An example of this is shown in Ref. 21. In addition, values of wall pressures and temperatures located off center were the same as the center values.

Impact-probe profiles are presented in Figs. 3 and 4 for air injection and in Figs. 5 and 6 for helium injection. The flow was probed at several axial locations that occurred during different experimental runs. While probing at a single location, the stagnation pressure of the injectant varied to within ±3.8% of the mean value. For profiles at a single injectant Mach number, the difference between the mean value of the injectant stagnation pressure for each profile was less than ±5%. In both the air and helium studies at low-injection Mach numbers, the first station measured is not at the exit of the slot ($x/s = 0$) but downstream of the slot shock structure at $x/s = 3$.

Because the upper wall of the injection nozzle is slanted at a 10-deg angle, the flow issuing out of the half-nozzle is radial with a maximum radial velocity at the tip of the nozzle. The interaction between the injectant and the freestream flows produced a lip shock in both streams. The injectant shock wave interacts with its thin boundary layer, causing it to separate, but reattachment soon fol-

Table 1 Experimental parameters

Case	Fluid	$T_{ti}/T_{t\infty}$	M_i	λ	u_i/u_∞	$(\rho u^2)_i/(\rho u^2)_\infty$	Re_s
1	Air	1	1.2	0.39	0.6	0.23	3.66×10^3
2	Air	1	2.2	0.87	1.0	0.87	1.2×10^4
3	Helium	1	1.3	0.19	1.9	0.36	1.87×10^3
4	Helium	1	2.2	0.41	2.4	0.98	6.34×10^3
5	Air	1.14	1.2	0.36	0.7	0.25	3.07×10^3
6	Air	1.14	2.2	0.82	1.0	0.82	1×10^4
7	Air	1.33	2.2	0.75	1.1	0.82	8.04×10^3
8	Helium	1.14	1.3	0.17	2.0	0.34	1.56×10^3
9	Helium	1.36	1.3	0.16	2.2	0.35	1.27×10^3
10	Helium	1.22	2.2	0.37	2.7	1.00	4.7×10^3

lows. This shock interaction has a small effect on the value of the adiabatic wall temperature, since the values downstream of the interaction region were close to the recovery value.[4] When the pitot pressure profile at the slot exit is measured, the physical presence of the probe affects the flow near the wall, since the size of the probe is large compared with the boundary layer of the slot flow.

In the case of the Mach 1.2 air injection shown in Fig. 3 for x/s = 3, 41, 58, and 96, the total pressure of the injectant is small compared with the freestream, $P_{ti}/P_{t\infty} = 0.18$. At $x/s = 3$, the profile clearly shows the slot flow and the freestream boundary layer as they are starting to mix. The sudden change in the profile at $y \approx 3.8$ mm is due to the probe passing the lip shock. By $x/s = 41$, the flat section of the injection profile has disappeared, indicating that the shear layer emanating from the lip has merged with the injectant boundary layer. For the profiles corresponding to $x/s = 58$ and 96, the pressure profiles for $y < 2$ mm appear to match the profiles at $x/s = 41$. At these downstream axial locations, the pressure profiles for $y > 4$ mm resemble the pressure variation for $y > 3$ mm at the axial location $x/s = 41$. In addition, these pressure profiles resemble the original freestream boundary-layer profile that is shown more clearly at $x/s = 0$ in Fig. 4. This comparison suggests that this region of the flow has not participated in the mixing process, but has been transversely displaced by the injectant. This behavior seems to be apparent for all cases tested.

The profiles for the air injection at $M_i = 2.2$ are shown in Fig. 4 for three axial locations, x/s = 0, 55, and 93. The ratio of the injectant total pressure to the freestream value measured at the end of the test rhombus is $P_{ti}/P_{t\infty} = 0.63$, which is closer to that for the freestream than that for the Mach 1.2 injection test. The profile at the exit of the slot near the wall is indented. This indentation, which

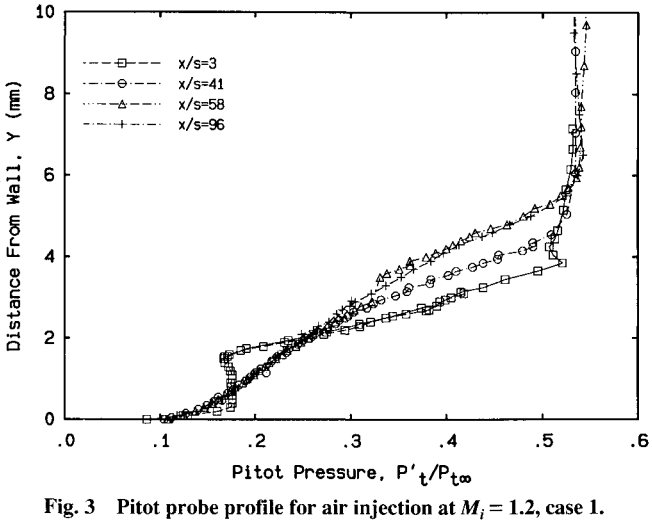

Fig. 3 Pitot probe profile for air injection at $M_i = 1.2$, case 1.

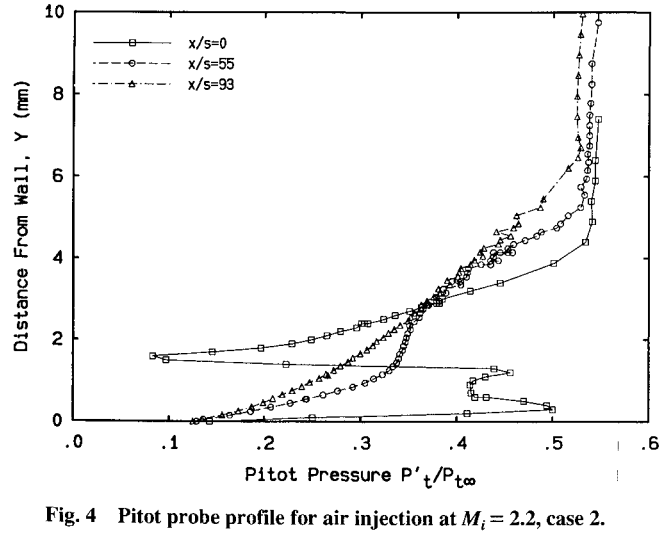

Fig. 4 Pitot probe profile for air injection at $M_i = 2.2$, case 2.

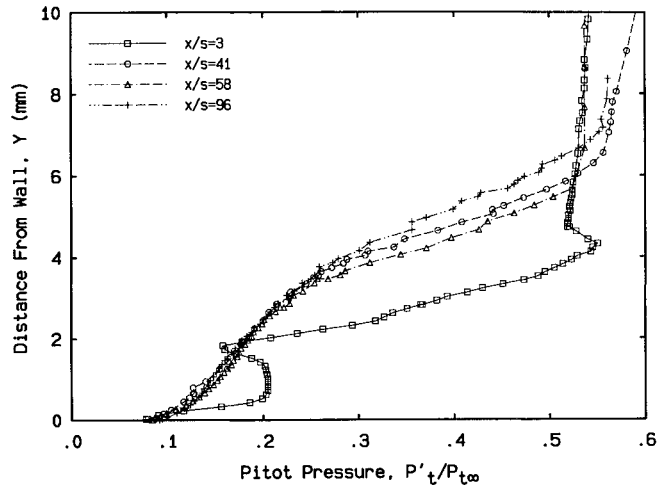

Fig. 5 Pitot probe profile for air injection at $M_i = 1.3$, case 3.

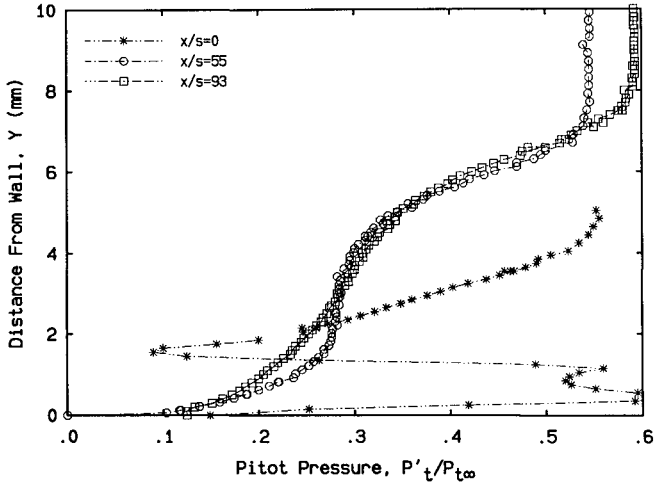

Fig. 6 Pitot probe profile for air injection at $M_i = 2.2$, case 4.

is also seen in Peak's work, is a result of the probe interaction with injectant boundary layer. As the probe approaches the wall, the probe's detached shock interacts with the injectant boundary layer. This interaction increases as the probe approaches the wall, causing the boundary layer to separate and the pressure to rise. The indentation was first suspected of being a result of the slot geometry. However, a closer look indicated that any adverse effect due to the geometry would have induced a profile that had the opposite trend than that found by probing. In the cases of the Mach 2.2 and 1.2 injection, the radius of curvature to throat height is 13 and 7, respectively, exceeding values recommended for supersonic nozzles.[22] The indentation does not appear in the Mach 1.2 case and is reduced as the Mach number is lowered.[21] Although the exit plane of the Mach 1.2 injection case is located closer to the curved surface than that of the Mach 2.2 injection, the distortion due to geometry should have been more severe than in the Mach 2.2 injection case.

The wake from the lip and the freestream boundary layer are more visible than in the preceding case, since in this case the first station is measured at the slot exit. By 50 slot heights the shear layer has merged with the injectant boundary layer, and the flow continues to form a boundary-layer-type flow. As with the lower Mach number case, after $x/s = 58$ the flow near the wall seems to be unchanged as the flow moves downstream. The profile for Mach 2.2 at $x/s = 90$ resembles the profile for Mach 1.2 at $x/s = 58$. For a given axial location downstream of the slot, the width of the viscous layer is slightly larger for $M_i = 2.2$ injection than for $M_i = 1.2$ injection.

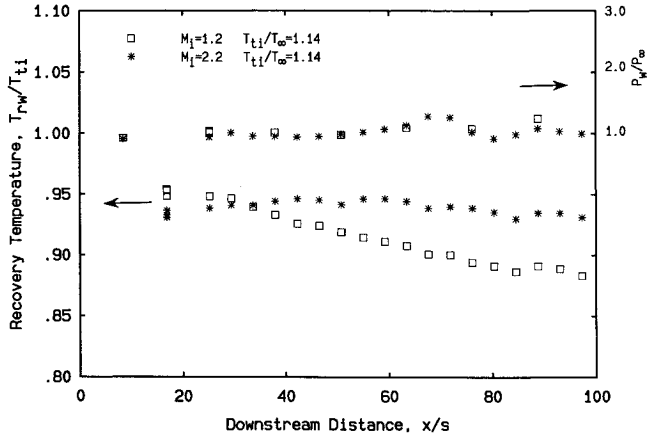

Fig. 7 Heated air injections pressure and temperature ratios, cases 5 and 6.

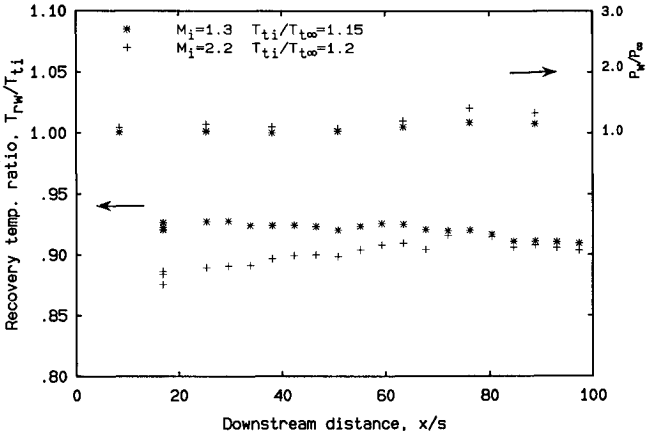

Fig. 8 Heated helium injections pressure and temperature ratios, cases 8 and 10.

In the case of the Mach 1.3 helium injection in Fig. 5, similar behavior to the air injection of Mach 1.2 is observed for the flow development near the wall. The total pressure in the jet is $P_{ti}/P_{t\infty} = 0.2$. The boundary layer of the injectant leaving the slot is larger in this case than for the Mach 1.2 air injection. The shear layer in the case of helium injection is also larger than for air, which is due to the higher velocity difference between the injectant and the freestream.

In Fig. 6, the injection of helium at $M_i = 2.2$ shows a similar profile at the exit of the slot as compared with that for air at $M_i = 2.2$. The injectant impact pressure is near that of the freestream with a total pressure ratio of $P_{ti}/P_{t\infty} = 0.7$. By 55 slot heights, the shear layer merges with the injectant boundary layer. The flatness of the impact-probe profile at the lower part of the lower layer is due to the high-injectant total pressure and not due to the helium stream persistence at that location. The viscous layer in this case is larger than that of both air injection cases and slightly larger than the Mach 1.3 helium injection case.

For all of the studies, the freestream profile shows that the value of the pitot pressure is nearly the same at all stations, indicating that the shock waves propagating through the flow are weak.

Wall Pressures and Temperatures Without Shock Interaction

Before examining the experimental results obtained with an impinging oblique shock, we made measurements of the wall static pressure and the adiabatic wall temperature with injection at the two different Mach numbers. Figures 7 and 8 show the distribution in wall static pressure normalized by the freestream static pressure, P/P_∞, and the recovery temperature normalized by the total temperature of the injected gas, T_{rw}/T_{ti}.

For air injection as shown in Fig. 7, the wall static pressure is fairly constant over the first 60 slot heights. There is an increase near $x/s \approx 70$, which is due to the reflected lip shock impinging on the wall. The pressure profile also indicates an adverse pressure gradient associated with injection, which increases with the injection Mach number. The wall temperatures were measured for approximately the same total injection temperature ($T_{t\infty} = 342$ K). The temperature distribution for $M_i = 1.3$ decreases with downstream distance as the injected fluid begins to mix with the freestream at $T_{t\infty} \approx 300$ K. However, the recovery temperatures corresponding to $M_i = 2.2$ show an increase over the first 40 slot heights. In this region of the flow, the total pressure profiles, as shown in Figs. 3 and 4, are considerably different due to the difference in injection velocity and Mach number. For flows at different Mach numbers and at the same total temperature, the recovery temperature is lower for the higher Mach number flow. Hence, the recovery temperature for $M_i = 2.2$ is lower than for $M_i = 1.3$ in the region of the flow just downstream of the nozzle.

The helium results as shown in Fig. 8 are similar to those for air injection. The wall static pressure with fluid injection increased at $x/s = 60$ due to the impingement of the reflected lip shock at that location. The overall pressure increase is larger for the injection at $M_i = 2.2$ than for that at $M_i = 1.3$ and is slightly larger than the pressure gradient associated with air injection. For $x/s < 80$, the recovery temperature is higher for $M_i = 1.3$ than for $M_i = 2.2$. This difference can again be attributable to the difference in injection Mach number. As compared with the air results, the downstream distance is considerably longer over which the $M_i = 2.2$ temperatures are lower than the $M_i = 1.3$ results. For axial locations corresponding to $x/s \geq 80$, the wall temperatures are approximately the same; how-

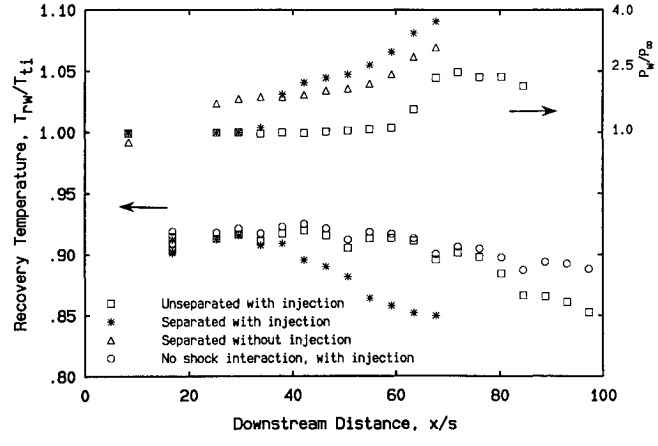

Fig. 9 Shock interaction with heated air injection at $M_i = 2.2$, $T_{ti}/T_{t\infty} = 1.33$, case 7.

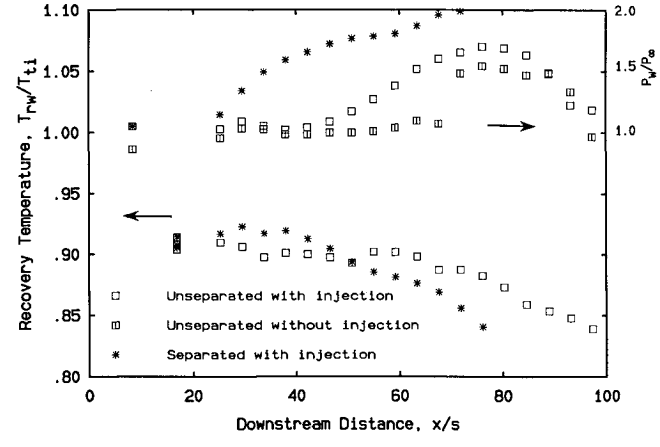

Fig. 10 Shock interaction with heated air injection at $M_i = 1.3$, $T_{ti}/T_{t\infty} = 1.36$, case 9.

ever, this similarity may be a result of the slight difference in total temperature of the injectants. Further downstream the $M_i = 1.3$ temperatures decrease more rapidly than for $M_i = 2.2$.[4] In addition, the recovery temperature appears to increase in the region where the lip shock impinges on the flow; the increase is expected since the shock wave decelerates the flow and the drop in the flow velocity results in an increase in the recovery temperature. However, this effect was not observed with the air experiments.

As discussed in the Background section, models that are developed to predict film cooling (or film heating, as in the present experiments) should incorporate the variations in the flow profiles. Using the definition given in Eq. (2), the effectiveness would be unity over the axial distance in which the recovery temperature equals that of the injectant. However, as shown in Figs. 7 and 8 for $M_i = 2.2$, the recovery temperature initially increases, which would result in an effectiveness greater than unity. The temperature rise is attributed to the merging of the injectant boundary layer and the wake emanating from the lip.[21] This region of the flow is determined by the behavior of the injectant jet. Farther downstream the effectiveness decreases from unity; in this region the wall temperatures are determined by the mixing process.

Wall Pressures and Temperatures with Shock Interaction

Figures 9–12 demonstrate the effects of an oblique shock wave on the film-heated flows. The results in Figs. 9–11 were obtained by measuring the wall static pressure and the equilibrium wall temperatures for a flow with and without injection in the presence of an impinging shock. Separation due to shock wave impingement was determined by 1) inspection of the wall pressure distribution for the presence of an inflection point and 2) using the schlieren system. The type of separation discussed in this study is what has been termed "effective" separation, which refers to the onset of the most dramatic change in the flowfield.[23] In several instances the tunnel unstarted just downstream of the interaction region. Since the separation process does not depend on the downstream conditions, only the recompression region is distorted by the tunnel unstart and not the strength of the leading reflected shock wave. In these cases, the data in the distorted region of the interaction are not shown in the plots. For one of the data sets in each figure, the shock strength was less than that required to produce separation in the flow. For this shock strength, the distribution in the wall static pressure and temperature was recorded, and then the injected flow was stopped. After the flow equilibrated and without a change in the angle of attack of the wedge, the wall static pressure distribution was measured without injection. A subsequent experiment was also run for the same injection conditions, but with a slightly larger angle of attack so that the shock strength was large enough to separate the flow. The strength of the weaker shock is then seen as the strength at incipient separation. To compare incipient separation with and without injection, an experiment without injection showed that the

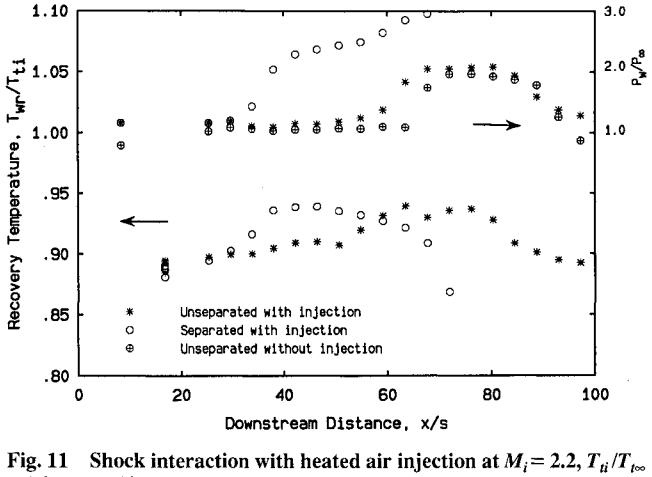

Fig. 11 Shock interaction with heated air injection at $M_i = 2.2$, $T_{ti}/T_{t\infty} = 1.22$, case 10.

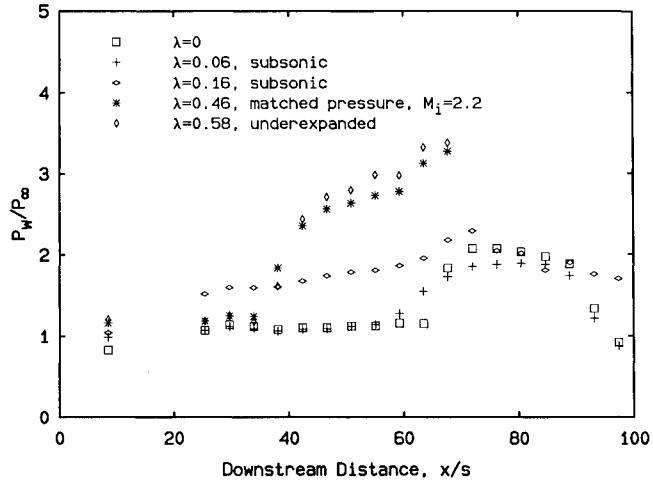

Fig. 12 Effect of isoenergetic helium injection on strong shock interaction.

boundary layer could withstand an increase in the pressure ratio up to a factor of 2.4 before separating.

For flow without injection, the shock wave caused by the nozzle step is weak and results in a change in freestream Mach number from 2.4 to 2.38. The boundary-layer profile just upstream of the interaction location is nearly identical to the profile just upstream of the slot. The step shock returns after impacting the wall opposite to the instrumented plate and intersects the expansion side of the wedge's surface, and it does not interfere with the shock wave emanating from the wedge. However, for the isobaric injections presented in this section the lip shock is stronger than the lip shock without injection. Moreover, on reflection from the opposite wall, the lip shock intersects with the shock wave caused by the wedge and increases its strength. This increase should be accounted for when comparing the shock interaction with and without injection.

Figure 9 shows the effect of shock-wave interaction with heated air injection at Mach 2.2. With injection, the flow did not separate for a pressure jump of 2.5, which is slightly higher than that required to separate the flow without injection. For a slightly larger wedge angle of attack, the flow separated as indicated in the figure by the pressure plateau. Also shown in the figure is the pressure distribution for the same angle of attack but without injection. In comparing the two pressure profiles with separation, the separation point with injection is about 20 slot heights further downstream, and the separation shock is stronger for the same angle of attack. A contribution to the increase in the peak pressure may result from the reflected lip shock intersecting with the shock generated by the wedge and increasing the intensity of the shock wave. The drop in the pressure distribution after 90 slot heights results from the expansion wave impinging on the wall from the trailing edge of the wedge. Also shown in the figure are the corresponding temperature distributions, as well as the distribution without shock impingement. For the flow with the weaker shock, the difference in the temperature measurements does not start until approximately $x/s = 80$, near the end of the interaction region. The difference in the temperatures in this region may also be a result of the expansion wave from the trailing edge of the wedge that is not present for the no-shock experiment. For the separated flow, the temperature difference begins when the pressure starts to increase; then the temperature decreases sharply with downstream distance.

Figure 10 presents similar results for heated helium injection at $M_i = 1.3$. Without injection, the shock wave impinging on the boundary layer results in an increase in the wall static pressure by a factor of 1.6. For the same angle of attack but with injection, the static pressure rise appears more gradual than that produced by the shock-wave/boundary-layer interaction obtained without injection. The upstream influence is larger than without injection, and the pressure jump with injection is higher. A slight increase in the

wedge angle of attack separated the injectant, indicating that the incipient pressure ratio is approximately 1.7, which is smaller than that obtained without injection. This indicates that injection-induced separation, which agrees with the finding of Holden et al.[19] With the stronger shock, the wall temperature shows an increase in the region further upstream and in approximately the same location as the beginning of the pressure increase. By the separation point, the temperature ratio begins to drop more quickly as compared with that resulting from the weaker shock.

Figure 11 shows the shock interaction with injection of heated helium at Mach 2.2. With injection and at incipient separation, the shock strength corresponds to a pressure rise of 2.0, which is higher than the incipient shock strength at the lower helium-injection Mach number. By comparing the pressure profiles in Figs. 5 and 6, the Mach 2.2 injection profile upstream of the interaction is fuller than that obtained by Mach 1.3 injection at $x/s = 60$. The figure shows that the rise in the pressure occurs more rapidly than for the $M_i = 1.3$ results, and there is a more significant temperature increase in this region. When the injection is stopped and without change in the wedge angle, the ratio of the pressure rise to the upstream pressure is 1.9, higher than for the $M_i = 1.3$ injection of 1.6. For the higher shock strength, the temperature distribution seems to follow the same pressure ratio distribution pattern and peaks where the pressure reaches its maximum. Even with injection at Mach 2.2, the flow still separates at a lower value than that without injection.

In both cases of helium injection, separation is induced, whereas in the case of air injection it is not. As shown in Table 1, the momentum flux for the Mach 2.2 helium injection condition is higher than the Mach 2.2 air injection condition, indicating that the prevention of separation is not solely a function of the momentum of the injected flow. An explanation can be deduced from the flow profiles of Figs. 4–6. Separation depends on the fullness of the velocity and Mach number profiles and the size of the subsonic portion of the incoming boundary layer. The air injection profile in Fig. 4 at the location nearest to the shock impingement location ($\approx x/s = 60$) is fuller than that of both helium injections. For the case of air injection at $M_i = 2.2$, using the Rayleigh formula and the profile at $x/s = 55$, we estimated the sonic line as being within 0.1 mm from the wall. In the case of helium injection at $M_i = 2.2$, the composition of the flow must be known to estimate the momentum flux and the location of the sonic point. If the flow is assumed to be entirely helium or entirely air, the sonic point for either case would be greater than 0.2 mm from the wall and the momentum flux of helium injection would be inferior to air injection. These comparisons suggest that the flow with air injection could withstand a stronger adverse pressure gradient.

If the interaction was next to the slot, as in Alzner and Zakkay,[16,17] the helium would have performed better than air in preventing separation, due to the greater momentum flux for the helium injection. However, if the interaction takes place farther downstream, the situation is different. Mixing between the freestream boundary layer and the injectant reduces the momentum of the injectant, and a new boundary layer is formed composed of the injectant and the freestream. Injecting a gas with a higher speed of sound increases the speed of sound and the subsonic region within the new boundary layer and makes it more prone to shock-wave separation. Similarly, in using hydrogen as a film coolant (as proposed for NASP), a problem is likely to develop farther downstream of the injectant slot, since hydrogen has a much higher speed of sound than air.

Figure 12 presents results for a shock wave of strength that can separate the helium injectant. The plot shows a number of isoenergetic helium injection rates starting with no injection up to a mass-flux ratio of $\lambda = 0.58$. The nozzle is positioned at the Mach 2.2 injection case. When the injection is increased to $\lambda = 0.063$, subsonic injection, the pressure rise is slightly reduced, but the upstream influence length is increased approximately twice. The first indication of separation occurs when the injection is increased to $\lambda = 0.16$. The influence length is large, nearly 60 slot heights. Since the upstream influence is a strong function of the size of the subsonic region of the incoming flow, it is conceivable that the injection of $\lambda = 0.16$ produces a large subsonic layer near the wall. Increasing the injection beyond $\lambda = 0.16$ results in a decrease of influence length, a decrease in the subsonic region near the wall. However, after injecting 25% over the isobaric injection ($\lambda = 0.46$), no reduction is observed.

Conclusions

The current experiments investigate the effects of shock-wave impingement on both air and helium injection. Two injection Mach numbers are examined for each fluid injection. The impact-pressure profiles are obtained for distances up to 90 slot heights.

The injection of the flow appears to lift the freestream boundary layer from the wall and transversely displace it. The upper part of the freestream boundary layer does not appear to participate in the mixing process. The higher velocity of the helium injection induces a larger wake than that of air injection; this has been shown to have an influence on the fullness of the profile at the shock impingement location. Helium injection also results in a larger boundary layer next to the wall than in the case of air.

At approximately 60 slot heights, a two-dimensional oblique shock is generated to impinge on the flow; the temperature measurements in this location of the flow indicate that the slot injection is beneficial for maintaining the surface at a desired temperature. However, with the shock impingement, the effectiveness of the film coolant decreases. In the experiments, the strength of the shock is varied to study flow with and without separation. Because the shock impingement is located well downstream of the injection nozzle, the experimental results cannot be directly compared with other experiments in which the shock impingement occurs much closer to the nozzle. It has been noted that discrepancies between previous studies are due to differences in the shape of the injectant profile at the shock impingement location, which is a function of downstream distance from the slot.

In the case of shock interaction, the helium injection is observed to induce separation. However, increasing the injection Mach number appears to delay separation. Air injection of Mach 2.2 is superior to both helium injection Mach numbers in preventing separation, even though its initial momentum flux is smaller than the Mach 2.2 helium injection. The induced separation in the case of helium injection has been attributed to the reduced fullness of its momentum flux just prior to the interaction, when compared to air or the original freestream boundary layer. The momentum flux at the shock impingement location is estimated to be larger for the air injection. Injecting a higher speed of sound fluid increases the speed of sound of the boundary layer, reducing the fullness of its Mach number profile, and therefore increasing its susceptibility to shock wave separation.

The effect of the shock interaction on the recovery temperature is more pronounced for the high-Mach-number helium case. When the injectant is separated, the recovery temperatures decrease more rapidly with downstream distance than the flows in which separation did not occur. However, as long as the flow remains attached, the influence of shock impingement on the recovery temperature is not large.

Acknowledgment

We would like to express our gratitude to E. E. Zukoski for his support, encouragement, and expertise during this investigation.

References

[1]Simoneau, R. J., Hendricks, R. C., and Gladden, H. J., "Heat Transfer in Aerospace Propulsion," *Proceedings of ASME National Heat Transfer Conference* (Houston, TX), Vol. 3, 1988, pp. 1–22.

[2]Kors, D. L., and Kissinger, R. D., "The Challenge of Demonstrating the X-30," *Aerospace America*, Vol. 28, No. 7, 1990, pp. 22–24.

[3]Kamath, P. S., Holden, M. S., and McClinton, C. R., "Experimental and Computational Study of the Effect of Shocks on Film Cooling Effectiveness in Scramjet Combustors," AIAA Paper 90-1713, June 1990.

[4]Juhany, K. A., Hunt, M. L., and Sivo, J. M., "Influence of Injectant Mach Number and Temperature on Supersonic Film Cooling Effectiveness," *Journal of Thermophysics and Heat Transfer*, Vol. 8, No. 1, 1994

(to be published).

[5]Goldstein, R. J., "Film Cooling," *Advances in Heat Transfer,* Vol. 7, 1971, pp. 321–380.

[6]Seban, R. A., and Back, L. H., "Velocity and Temperature Profiles in Turbulent Boundary Layer With Tangential Injection," *Journal of Heat Transfer,* Vol. 84, No. 2, 1962, pp. 45–54.

[7]Launder, R. E., and Rodi, W., "The Turbulent Wall Jet, Measurements and Modeling," *Annual Review of Fluid Mechanics,* Vol. 15, 1983, pp. 429–459.

[8]Seban, R. A., and Back, L. H., "Velocity and Temperature Profiles in a Wall Jet," *International Journal of Heat and Mass Transfer,* Vol. 3, No. 4, 1961, pp. 255–266.

[9]Delery, J. M., "Shock Wave Turbulent Boundary Layer Interaction and Its Control," *Progress in Aerospace Sciences,* Vol. 22, No. 4, 1985, pp. 209–280.

[10]Peak, D. J., "The Use of Air Injection to Prevent Separation of the Turbulent Boundary Layer in Supersonic Flow," British Ministry of Aviation, Aeronautical Research Council, C.P. No. 890, 1966.

[11]Grin, V. T., and Zakharov, N. N., "Experimental Investigation of the Effect of Tangential Blowing and Wall Cooling on Flow with Separation," *Fluid Dynamics,* Vol. 6, No. 6, 1974, pp. 1035–1038.

[12]Yates, C. L., "Two-Dimensional, Supersonic Mixing of Hydrogen and Air Near A Wall," NASA CR-1793, March 1971.

[13]Walker, D. A., Campbell, R. L., and Schetz, J. A., "Turbulence Measurements for Slot Injection in Supersonic Flow," AIAA Paper 88-0622, Jan. 1990.

[14]Hyde, C. R., Smith, B. R., Schetz, J. A., and Walker, D. A., "Turbulence Measurements for Heated Gas Slot Injection in Supersonic Flow," *AIAA Journal,* Vol. 28, No. 9, 1990, pp. 1605–1614.

[15]Kwok, F. T., Andrew, P. L., and Ng, W. F., "An Experimental Investigation of a Supersonic Shear Layer with Slot Injection of Helium," AIAA Paper 90-0093, Jan. 1990.

[16]Alzner, E., and Zakkay, V., "Turbulent Boundary Layer Shock Interaction with and without Injection," Aeronautical Research Labs, ARL 70-0092, June 1970.

[17]Alzner, E., and Zakkay, V., "Turbulent Boundary Layer-Shock Interaction with and without Injection," *AIAA Journal,* Vol. 9, No. 9, 1971, pp. 1769–1776.

[18]Ledford, O. C., and Stollery, J. L., "Film Cooling of Hypersonic Inserts," Imperial College, Aero Rept. 72-15, London, July 1972.

[19]Holden, M. S., Nowak, R. J., Olsen, G. C., and Rodriguez, K. M., "Experimental Studies of Shock Wave/Wall Jet Interaction in Hypersonic Flow," AIAA Paper 90-0607, Jan. 1990.

[20]Olsen, G. C., Nowak, R. J., Holden, M. S., and Baker, N. R., "Experimental Results for Film Cooling in 2-D Supersonic Flow Including Coolant Delivery Pressure, Geometry, and Incident Shock Effects," AIAA Paper 90-0605, Jan. 1990.

[21]Juhany, K. A., "Supersonic Film Cooling Including the Effect of Shock Wave Interaction," Ph.D. Dissertation, Dept. of Aeronautics, California Inst. of Technology, Pasadena, CA, 1993.

[22]Pope, A., and Goin, K. L., *High-Speed Wind Tunnel Testing,* Wiley, New York, 1965, p. 44.

[23]Delery, J., and Marvin, J. G., "Shock-Wave Boundary Layer Interactions," edited by E. Reshotko, AGARD-AG-280, Feb. 1986.